IQC-based robust stability analysis for LPV control of doubly-fed induction generators

Tien, H. N.; Scherer, C. W.; Scherpen, J. M. A.

Published in:
Proceedings of the 10th International Conference on Control, Automation, Robotics and Vision, ICARCV 2008

Publication date:
2008

2008 10th Intl. Conf. on Control, Automation, Robotics and Vision
Hanoi, Vietnam, 17–20 December 2008

IQC-based robust stability analysis for LPV control of doubly-fed induction generators

H. Nguyen Tien*, C. W. Scherer*, J. M. A. Scherpen**
*Delft Center for Systems and Control, Delft University of Technology, The Netherlands
**Faculty of Mathematics and Natural Sciences, University of Groningen, The Netherlands

***Abstract*—Parameters of electrical machines are usually varying with time in a smooth way due to changing operating conditions, such as variations in the machine temperature and/or the magnetic saturation. This paper is concerned with robust stability analysis of controlled Doubly-Fed Induction Generators (DFIGs) that takes into account the time-varying nature of the parameter variations as well as bounds on their rate-of-variations. First, a self-scheduled Linear Parameter Varying (LPV) current controller design for the inner rotor-side loop is presented. The design is based on viewing the mechanical angular speed as an uncertain yet online measurable parameter and on subsuming the problem into the framework of LPV controller synthesis. Then the parameter-dependent model of the machine is transform into a Linear Fractional Representation, which allows to perform a stability analysis based on a specifically chosen set of Integral Quadratic Constraints (IQCs). Some simulation and analysis test results are given to demonstrate the robustness margins that result with this control algorithm.**

***Index Terms*—Doubly-fed induction generator (DFIG), linear parameter varying (LPV) systems, slowly time-varying parameter, robust stability, integral quadratic constraints (IQC).**

I. Introduction

Doubly-fed induction machines (DFIMs) are often used as generators for variable speed wind turbines because of their advantages in comparison with other machines. The most important feature is that approximately 30% of the generator power is handled by power converters. Therefore, converters should be designed in a cost effective fashion.

In the literature, conventional control designs for DFIMs are often relying on a nominal machine model under the hypothesis that the machine parameters are precisely known. This motivates the application of more advanced control synthesis techniques in order to improve system performance against changes in the machine parameters and exogenous inputs. More specifically, an H_∞ control approach is proposed for induction generators in [1], [2] and for induction motor control in [3], [4], [5]. Recently, the LPV current control approach, which takes the parameter variations into account directly in the control design, is applied for an induction motor in [6], [7]. In the latter reference, the electrical angular rotor speed and the estimated magnetizing current are considered to be varying parameters. The control objective is to track references for the magnetizing current and the angular electrical rotor speed. A quasi-LPV approach is applied to the design of a stator current controller and a speed controller. In [6], the same method is employed for the inner current control loop, and the LPV controller synthesis is extended to a discrete time setting. Robustness of such controlled systems can be demonstrated by means of simulation for several given values of the respective uncertain parameters [8], [5], [3]. Since such simulation results are not sufficient to confirm robustness, the structured singular value tool can be used for robustness analysis against Linear Time-Invariant (LTI) uncertainties [9]. For Linear Time-Varying (LTV) parametric uncertainty, robustness analysis can be based on parameter-dependent Lyapunov functions if the system is dependening affinely on slowly-varying parameters [10], [11]. As an extension of the classical multiplier theory, the Integral Quadratic Constraints (IQCs) approach [12], [13] provides a flexible way for robust stability analysis with both rate-bounded LTV parametric and dynamic uncertainties.

In this paper, the machine inductances and the rotor's mechanical angular speed are considered as slowly-varying parameters, and an IQC-based robust stability test is applied for the LPV current controller that is designed for a nominal machine model. In Section II we first present the synthesis of a gain-scheduled current controller for DFIGs, and we show experimental results in order to demonstrate that the LPV controller achieves the desired tracking performance requirements [14]. In Section III we discuss possible situations that might cause changes in the values of the machine parameters. The IQC-based robust stability test is stated in Section IV, in which we also present our main analysis results. Section V contains some conclusions.

II. Synthesis of gain-scheduled current controller

A. The nominal machine model

In this paper, a dq reference frame, which is independent of the machine parameters and the rotor speed measurement accuracy, is adopted. This reference frame has the d axis coinciding with the grid voltage vector [15]. In this reference frame, the DFIG equations can be written as

$$\begin{aligned} \dot{x}_r &= A_{rc}(\omega)x_r + B_{rc}v_{rs} \\ y_r &= C_{rc}x_r \end{aligned} \tag{1}$$

where $x_r = \begin{pmatrix} i_{rd} & i_{rq} & \Psi_{sd} & \Psi_{sq} \end{pmatrix}^T$; $v_{rs} = \begin{pmatrix} v_s & v_r \end{pmatrix}^T$; $v_s = \begin{pmatrix} v_{sd} & v_{sq} \end{pmatrix}^T$; $v_r = \begin{pmatrix} v_{rd} & v_{rq} \end{pmatrix}^T$; $y_r = \begin{pmatrix} i_{rd} & i_{rq} \end{pmatrix}^T$;

$$A_{rc}(\omega) = \begin{pmatrix} a_{11} & \omega_s - \omega_m & \frac{a_{13}}{T_s} & -a_{13}\omega_m \\ \omega_m - \omega_s & a_{11} & a_{13}\omega_m & a_{13} \\ a_{31} & 0 & a_{33} & \omega_s \\ 0 & a_{31} & -\omega_s & a_{33} \end{pmatrix}; \quad (2)$$

$$B_{rc} = \begin{pmatrix} -\frac{a}{L_m} & 0 & \frac{a+1}{L_r} & 0 \\ 0 & -\frac{a}{L_m} & 0 & \frac{a+1}{L_r} \\ 1 & 0 & 0 & 0 \\ 0 & 1 & 0 & 0 \end{pmatrix}; \quad (3)$$

$$C_{rc} = \begin{pmatrix} 1 & 0 & 0 & 0 \\ 0 & 1 & 0 & 0 \end{pmatrix}; \quad (4)$$

$a_{11} = -\left(\frac{a+1}{T_r} + \frac{a}{T_s}\right)$; $a_{13} = \frac{a}{L_m}$; $a_{31} = \frac{L_m}{T_s}$; $a_{33} = -\frac{1}{T_s}$; $a = \frac{1-\sigma}{\sigma}$; $T_s = \frac{L_s}{R_s}$ and $T_r = \frac{L_r}{R_s}$ denote the time constants of the stator and rotor; $v_{sd}, v_{sq}, v_{rd}, v_{rq}, i_{sd}, i_{sq}, i_{rd}, i_{rq}$ are voltage and current components of the stator and rotor respectively; Ψ_{sd}, Ψ_{sq} are the stator flux components; L_s, L_r are the stator and rotor inductances; L_m is the mutual inductance; R_s, R_r are the stator and rotor resistances; $\sigma = 1 - \frac{L_m^2}{L_s L_r}$ is the total linkage coefficient; $\omega_m = \omega_s - \omega_r$ is the mechanical angular velocity of the rotor; ω_s is the electrical angular velocity of the stator (or grid); and ω_r is the electrical angular velocity of the rotor.

B. The current control loop

The rotor current control loop with controller K_{rc} is depicted in Fig. 1. The design goal of the rotor current controller K_{rc} is to achieve high dynamic performance and robust tracking of the rotor currents. In Fig. 1, G_{rc} represents the plant according to equations (1).

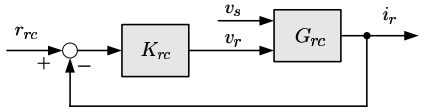

Fig. 1. The current control loop

C. The current controller synthesis

In this section we briefly address the LPV current controller synthesis problem. More details about designing the continuous-time LPV current controller for DFIGs can be found in [16]. Questions concerning the discretization of the continuous-time LPV controller and the implementation in a real setup are presented in [14].

The mechanical angular speed of the DFIG can be expressed as $\omega_m = \omega_s(1 + p_\omega \delta_\omega)$, where $-1 \leq \delta_\omega \leq 1$ and $p_\omega = 0.3$. Hence (1) becomes affinely parameter dependent and can be rewritten as

$$\dot{x}_r = (A_{rr} + \delta_\omega A_{r\omega})\, x_r + B_s v_s + B_r v_r \quad (5)$$

where $A_{rr}, A_{r\omega}$ are matrices defined by

$$A_{rr} = \begin{pmatrix} a_{11} & 0 & \frac{a_{13}}{T_s} & -a_{13}\omega_s \\ 0 & a_{11} & a_{13}\omega_s & \frac{a_{13}}{T_s} \\ a_{31} & 0 & a_{33} & \omega_s \\ 0 & a_{31} & -\omega_s & a_{33} \end{pmatrix};$$

$$A_{r\omega} = \begin{pmatrix} 0 & -\omega_s p_\omega & 0 & -\frac{a\omega_s p_\omega}{L_m} \\ \omega_s p_\omega & 0 & \frac{a\omega_s p_\omega}{L_m} & 0 \\ 0 & 0 & 0 & 0 \\ 0 & 0 & 0 & 0 \end{pmatrix}.$$

The interconnection of the system used for synthesis is shown in Fig. 2. The external disturbance input w_{rc} consist of the stator voltages and the reference rotor currents $w_{rc} = \begin{pmatrix} v_{sd} & v_{sq} & i_{rd}^{ref} & i_{rq}^{ref} \end{pmatrix}^T$. The controller outputs are $v_r = \begin{pmatrix} v_{rd} & v_{rq} \end{pmatrix}^T$. The controller inputs are the tracking errors which equal $e_r = \begin{pmatrix} e_{rcd} & e_{rcq} \end{pmatrix}^T = \begin{pmatrix} i_{rd}^{ref} - i_{rd} & i_{rq}^{ref} - i_{rq} \end{pmatrix}^T$. The controlled outputs are $y_r = \begin{pmatrix} i_{rd} & i_{rq} \end{pmatrix}^T$.

The weighting function $W_{rs} = \begin{pmatrix} W_{rsd} & 0 \\ 0 & W_{rsq} \end{pmatrix}$ used for the controller synthesis is kept small over the low frequency range for disturbance attenuation of the stator voltages. The first-order high-pass filter $W_{rt} = \begin{pmatrix} W_{rtd} & 0 \\ 0 & W_{rtq} \end{pmatrix}$ is used to keep the closed loop bandwidth at a desired value and to shape the complementary sensitivity function.

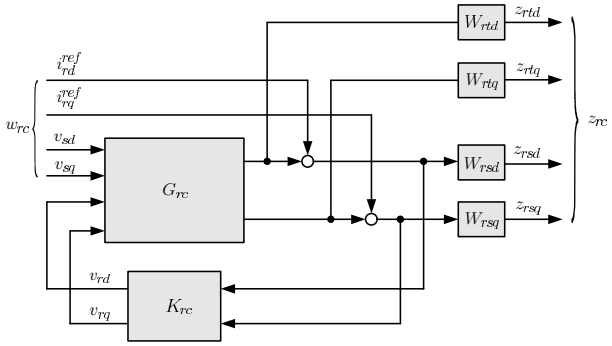

Fig. 2. The interconnection of the system

The optimization problem is to find a stabilizing controller of the form

$$\begin{pmatrix} \dot{x}_c(t) \\ u_c(t) \end{pmatrix} = \begin{pmatrix} A_c(\omega_m(t)) & B_c(\omega_m(t)) \\ C_c(\omega_m(t)) & D_c(\omega_m(t)) \end{pmatrix} \begin{pmatrix} x_c(t) \\ y_c(t) \end{pmatrix} \quad (6)$$

such that the closed-loop system of Fig. 2, which admits the description

$$\begin{pmatrix} \dot{\xi}_{rc}(t) \\ z_{rc}(t) \end{pmatrix} = \begin{pmatrix} \mathcal{A}_{rc}(\omega_m(t)) & \mathcal{B}_{rc}(\omega_m(t)) \\ \mathcal{C}_{rc}(\omega_m(t)) & \mathcal{D}_{rc}(\omega_m(t)) \end{pmatrix} \begin{pmatrix} \xi_{rc}(t) \\ w_{rc}(t) \end{pmatrix},$$

is internally stable and the L_2-gain of the channel $w_{rc} \rightarrow z_{rc}$ is smaller than a specified bound γ for all trajectories $\omega_m(.)$ that satisfy $\omega_m(t) \in [\omega_{min}, \omega_{max}] = [(1-p_\omega)\omega_s, (1+p_\omega)\omega_s]$.

We employ the Linear Matrix Inequality (LMI) Control Toolbox in Matlab [17] in order to compute the vertex controllers

$$K_{rc1} = \begin{pmatrix} A_{Krc1} & B_{Krc1} \\ C_{Krc1} & D_{Krc1} \end{pmatrix}, \quad K_{rc2} = \begin{pmatrix} A_{Krc2} & B_{Krc2} \\ C_{Krc2} & D_{Krc2} \end{pmatrix}$$

in a polytopic controller description. Then the controller is implemented as follows: for a value $\omega_m(t)$ measured at time t, we use

$$K_{rc}(t) = \frac{\delta_w^{max} - p(t)}{\delta_w^{max} - \delta_w^{min}} K_{rc1} + \frac{p(t) - \delta_w^{min}}{\delta_w^{max} - \delta_w^{min}} K_{rc2} \qquad (7)$$

with $\delta_w^{max} = 1$, $\delta_w^{min} = -1$, and $p(t) = \frac{\omega_m(t) - \omega_s}{\omega_s p_w}$ for simulating the controller dynamics.

D. Experimental results

In the laboratory test model, an 11kW induction machine was used as the prime mover. An 4kW doubly-fed induction generator was used for all experiments. Fig. 3 shows the performance of the inner current-control loop corresponding to step changes of the rotor currents i_{rd} and i_{rq}. The rotor speed is set to 1350 rpm. The reference value of the d-component of the rotor current is set to perform a sudden step from $0A$ to $1.5A$ while the q-component of the rotor current is kept at $0A$ as shown on the left of Fig. 3. Similarly, as on the right of Fig. 3, the reference value of the q-component of the rotor current is set to perform a sudden step from $0A$ to $-2A$ while the q-component of the rotor current is kept at $0A$. As we can see from Fig. 3, the LPV controller achieves good tracking of the references although the current measurements are corrupted by noise.

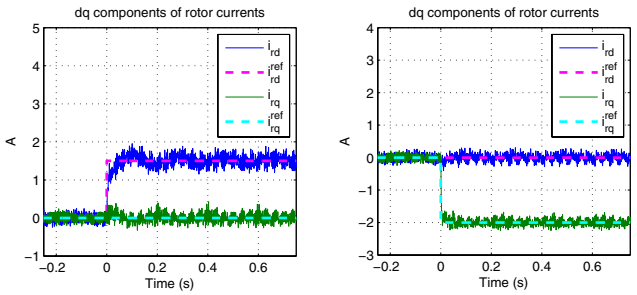

Fig. 3. Performance of the controlled system with step changes of i_{rd} (left) and i_{rq} (right)

III. The System Representation with Uncertainties

A. Parameter variations

The machine parameters can be considered as slowly time-varying parameters since their values depend naturally on slowly time-varying characteristics of the machine, namely temperature and magnetic saturation. The variations of the machine resistances R_s, R_r are mainly due to machine temperature changes. However, by simulation it can be verified that changes in the values of R_s and R_r do not cause significant changes in performance of the controlled system. Therefore, their variations will not be considered in the robust stability analysis of this paper.

The stator and rotor inductances L_s, L_r, and the mutual inductance L_m vary with the machine flux due to magnetic saturation and winding current modulus [18]. Since L_s, L_r, L_m, and the mechanical angular speed of the rotor ω_m are all bounded, the uncertainty set $\boldsymbol{\delta}$ of the parameter vector $\delta = (L_s, L_r, L_m, \omega_m)$ is taken to be the corresponding 4-dimensional cube, which is a polytope with $2^{\text{size}(\delta)} = 2^4 = 16$ generators:

$$\begin{aligned} \boldsymbol{\delta} \quad = \quad & co\left\{(L_s, L_r, L_m, \omega_m) : L_s \in \{\underline{L}_s, \overline{L}_s\}, L_r \in \{\underline{L}_r, \overline{L}_r\}, \right. \\ & \left. L_m \in \{\underline{L}_m, \overline{L}_m\}, \omega_m \in \{\underline{\omega}_m, \overline{\omega}_m\}\right\}. \end{aligned}$$

As will be presented in the next sections, robust stability analysis can be performed for a common variation of all parameters in this polytopic region. However, an investigations of closed-loop stability/performance subject to variations of individual machine parameters (while fixing the other three) is also useful in providing information about robustness of the controlled system in the controller design process. Fig. 4 shows, for instance, the closed-loop performance of the controlled system with respect to rotor inductance variations in the range of 95% to 125% of its nominal value. Fig. 4a - Fig. 4d show the Bode plots of the reference inputs i_r^{ref} and the stator voltages v_s to the outputs i_r and the control errors e_r, respectively. Fig. 4e - Fig. 4f depict the step responses from the reference inputs i_r^{ref} to outputs i_r and control errors e_r, respectively. It can be observed that, in the face of the uncertainty, the performance characteristics undergo some changes. Although the overshoots become larger, the system seems to remain robustly stable. This motivates a theoretically sound robust stability analysis as presented next.

B. Linear fractional representation of the system

Since the matrices of the state-space description (5) depend rationally on the machine inductances L_s, L_r, and L_m, it is not difficult to obtain a Linear Fractional Representation (LFR) of the plant.

We employ the Robust Control Toolbox in Matlab [19] in order to extract certain and uncertain components of the uncertain system. When we use the numerical reduction method in the robust control toolbox, which is similar to truncated balanced realizations, we note that the order of the uncertainty matrices will be reduced significantly.

The uncertainty matrix Δ_{rp} of the uncertain plant can be described as

$$\Delta_{rp} = \text{diag}\left(\delta_s I_{r_s}, \delta_r I_{r_r}, \delta_m I_{r_m}, \delta_\omega I_{r_\omega}\right), \qquad (8)$$

in which r_s, r_r, r_m, and r_ω are the dimensions of the uncertainty blocks corresponding to the machine inductances L_s, L_s, L_s and the rotor speed ω_m, respectively. The sizes of

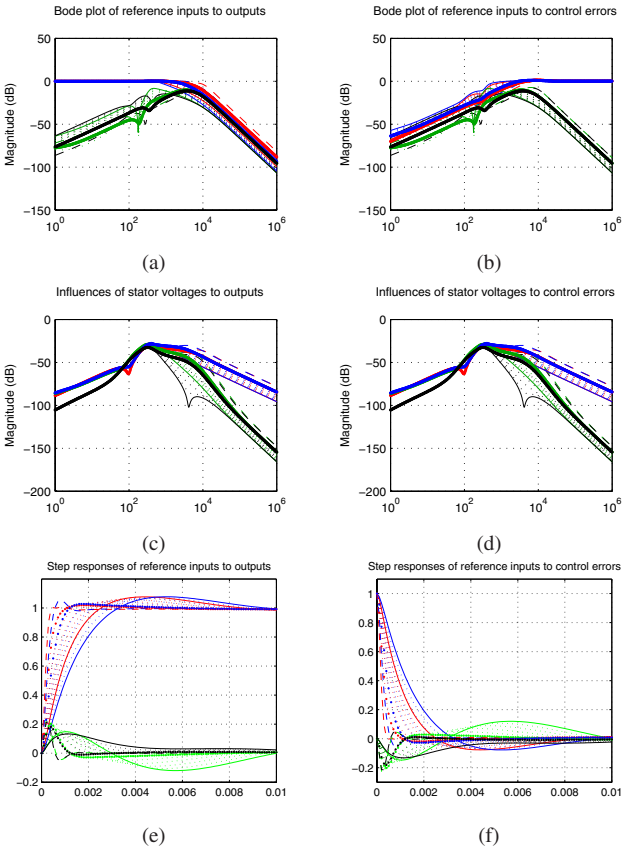

Fig. 4. Performance of the controlled system subject to the rotor inductance variations from 95% to 125% of its nominal value. (a) - (d) in frequency domain, (e) - (f) in time domain characteristics. Thick lines, dashed lines, solid lines, and dotted lines correspond with nominal, minimum, maximum, and intermediate values of the varying parameter, respectively.

TABLE I
UNCERTAINTIES AND MATRICES

Uncertainties	Uncertainty matrix Δ_{rp} size
L_s	4×4 ($r_s = 4$, $r_r = 0$, $r_m = 0$, $r_\omega = 0$)
L_r	2×2 ($r_s = 0$, $r_r = 2$, $r_m = 0$, $r_\omega = 0$)
L_m	6×6 ($r_s = 0$, $r_r = 0$, $r_m = 6$, $r_\omega = 0$)
ω_m	8×8 ($r_s = 0$, $r_r = 0$, $r_m = 0$, $r_\omega = 0$)
L_s and ω_m	8×8 ($r_s = 4$, $r_r = 0$, $r_m = 0$, $r_\omega = 4$)
L_r and ω_m	6×6 ($r_s = 0$, $r_r = 2$, $r_m = 0$, $r_\omega = 4$)
L_m and ω_m	10×10 ($r_s = 0$, $r_r = 0$, $r_m = 6$, $r_\omega = 4$)

the resulting uncertainty matrices for different parameters are summarized in Table I. The LFR of the plant and the LPV rotor current controller as well as the interconnection of the closed-loop system is depicted in Fig. 5.

The LFT representation of the LPV controller is constructed similarly. From the polytopic controller description (7) we have

$$K_{rc}^{lpv} = \frac{1-\delta_\omega}{2} K_{rc1} + \frac{\delta_\omega + 1}{2} K_{rc2}. \tag{9}$$

The resulting uncertainty matrix Δ_{rk} is

$$\Delta_{rk} = \delta_\omega I_6. \tag{10}$$

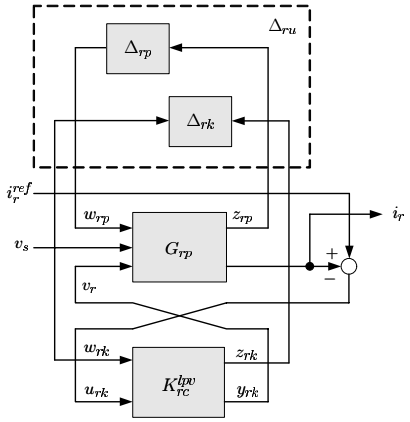

Fig. 5. The interconnection of the closed-loop controlled system

IV. ROBUSTNESS ANALYSIS

In this section the set of real symmetric matrices of dimension $m \times m$ is denoted by $\mathbb{S}^m$. Moreover, $\mathcal{L}_c^{m\times n}$ denotes the set of all causal linear operators that map $L_2^n[0,\infty)$ into $L_2^m[0,\infty)$. Recall that, roughly, an operator is causal if the past output (at any current time) is not affected by any modification of the future of the input signal. We refer to the set of stable and causal LTI systems by $\mathcal{RH}_\infty^{m\times n}$.

Let us now consider the standard setup for stability analysis, as given in Fig. 6, where $M \in \mathcal{RH}_\infty^{p\times p}$ is a known causal linear time-invariant operator and $\Delta \in \mathcal{L}_c^{p\times p}$ is a causal linear time-varying operator. For some set of uncertainties $\mathbf{\Delta} \subset \mathcal{L}_c^{p\times p}$ we say that M is robustly stable against $\mathbf{\Delta}$ if the feedback interconnection of M and Δ in Fig. 6 is well-posed and stable for all $\Delta \in \mathbf{\Delta}$.

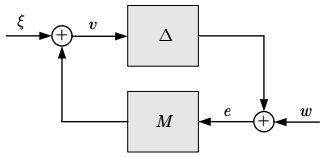

Fig. 6. The standard setup for robust stability analysis

For the standard set-up in Fig. 6, if Δ is a linear time-invariant system that is bounded as $||\Delta||_\infty \leq 1$, robust stability is guaranteed if $\|M\|_\infty < 1$. Furthermore, frequency dependent scalings can be used in order to arrive at a less conservative measure for robust stability if the uncertainties are structured. In case that $\Delta \in \mathcal{L}_c$ is a general LTV uncertainty with bounded L_2-gain, the scaling matrices need to be frequency-independent [20], [21]. However, static scalings are conservative if Δ results from structured parametric rate-bounded uncertainties as appearing in our DFIM model. An effective solution for such problems is to use the IQC approach for robust stability analysis as presented in the next part of this section.

A. IQC-based robust stability analysis

Theorem 1 (IQC stability [12]): Let $\Pi = \begin{pmatrix} \Pi_{11} & \Pi_{12} \\ \Pi_{12}^* & \Pi_{22} \end{pmatrix}$ be an IQC multiplier, a transfer matrix with $\Pi^* = \Pi$ that is bounded on the extended imaginary axis and that satisfies

$$\begin{pmatrix} I_p \\ \tau\Delta \end{pmatrix}^* \Pi \begin{pmatrix} I_p \\ \tau\Delta \end{pmatrix} \geq 0 \quad \forall \Delta \in \mathbf{\Delta}, \forall \tau \in [0,1]. \tag{11}$$

Then the feedback system of Fig. 6 is robustly stable against $\mathbf{\Delta}$ if the following conditions hold:

(i) $(M, \tau\Delta)$ is well-posed for all $\tau \in [0,1]$ and for all $\Delta \in \mathbf{\Delta}$.
(ii) There exists an $\epsilon > 0$ such that

$$\begin{pmatrix} M(j\omega) \\ I_p \end{pmatrix}^* \Pi(j\omega) \begin{pmatrix} M(j\omega) \\ I_p \end{pmatrix} \preceq -\epsilon I \quad \forall \omega \in [0, \infty). \tag{12}$$

Recall from [12] that the search for suitable multipliers Π in order to guarantee the frequency domain inequality (12) can be transformed into an LMI by employing the Kalman-Yakubovich-Popov (KYP) lemma [22], [23].

In this paper we apply a particular IQC test for LTV uncertainty that relies on the so-called swapping lemma [13], [24]. More specifically, we employ the following generalized version of this auxiliary result as given in [22].

Lemma 1 (Swapping lemma): Consider $\Delta_r = diag(I_{r_1} \otimes \delta_1, ..., I_{r_\nu} \otimes \delta_\nu) \in \mathbf{\Delta}$, together with $G_l = diag(G_1, ..., G_\nu)$, where $G_i = \left[\begin{array}{c|c} A_{G_i} & B_{G_i} \\ \hline C_{G_i} & D_{G_i} \end{array}\right] \in \mathcal{RH}_\infty^{l_i \times r_i}$, $A_{G_i} \in \mathbb{R}^{k_i \times k_i}$, $B_{G_i} \in \mathbb{R}^{k_i \times r_i}$, $C_{G_i} \in \mathbb{R}^{l_i \times k_i}$, $D_{G_i} \in \mathbb{R}^{l_i \times r_i}$ for $i = 1, .., \nu$, with A_{G_i} having all its eigenvalues in the open left-half plane. Let $\Delta_l \triangleq diag(I_{l_1} \otimes \delta_1, ..., I_{p_\nu} \otimes \delta_\nu)$, $V_\Delta \triangleq diag(I_{k_1} \otimes \dot{\delta}_1, ..., I_{k_\nu} \otimes \dot{\delta}_\nu)$, and define $G_B \triangleq diag(G_{B_1}, ..., G_{B_\nu})$, $G_C \triangleq diag(G_{C_1}, ..., G_{C_\nu})$ with

$$\begin{aligned} G_{B_i} &\triangleq (sI - A_{G_i})^{-1} B_{G_i} \\ G_{C_i} &\triangleq C_{G_i} (sI - A_{G_i})^{-1}. \end{aligned}$$

where $G_{B_i} \in \mathcal{RH}_\infty^{k_i \times r_i}$, and $G_{C_i} \in \mathcal{RH}_\infty^{l_i \times k_i}$. Then

$$G_{el} \Delta_{er} = \Delta_{el} G_{er} \tag{13}$$

where $G_{el} = \begin{pmatrix} G_l & G_C \\ 0 & I \end{pmatrix}$; $\Delta_{er} = \begin{pmatrix} \Delta_r \\ V_{\Delta_k} G_B \end{pmatrix}$; $\Delta_{el} = \begin{pmatrix} \Delta_l & 0 \\ 0 & V_{\Delta_k} \end{pmatrix}$; $G_{er} = \begin{pmatrix} G_l \\ G_B \end{pmatrix}$.

Based on this result let us introduce the abbreviations $L = \begin{pmatrix} G_{er} M_e \\ G_{el} \end{pmatrix} = \left[\begin{array}{c|c} A_L & B_L \\ \hline C_L & D_L \end{array}\right]$, where $M_e \triangleq \begin{pmatrix} M & 0_{r_e \times k_e} \end{pmatrix}$ with $r_e = \sum_{i=1}^\nu r_i$, and $k_e = \sum_{i=1}^\nu k_i$ is an extended version of the original system M and $A_L \in \Re^{d \times d}$ is stable. Define the set

$$\mathbf{\Delta}_e \triangleq \left\{ \begin{array}{c} \Delta_{er} = \begin{pmatrix} \Delta_r \\ V_{\Delta_k} G_B \end{pmatrix} \\ \Delta_r = diag(I_{r_1} \otimes \Delta_1, ..., I_{r_\nu} \otimes \Delta_\nu) \in \mathbf{\Delta}, \\ V_{\Delta_k} = diag(I_{k_1} \otimes \dot{\delta}_1, ..., I_{k_\nu} \otimes \dot{\delta}_\nu) \end{array} \right\}. \tag{14}$$

Then we note that, for $X_e \in \mathbb{S}^{n_e}$, $U_e \in \mathbb{S}^{n_u}$, and $Y_e \in \mathbb{R}^{n_e \times n_u}$, where $n_e = \sum_{i=1}^\nu (l_i + k_i)$, and $n_u = \sum_{i=1}^\nu (l_i + k_i)$, the inequality

$$\begin{aligned} 0 &\preceq \begin{pmatrix} I \\ \tau\Delta_{er} \end{pmatrix}^* \begin{pmatrix} G_{er}^* X_e G_{er} & G_{er} Y_e G_{el} \\ G_{el}^* Y_e^T G_{er} & G_{el}^* U_e G_{el} \end{pmatrix} \begin{pmatrix} I \\ \tau\Delta_{er} \end{pmatrix} \\ &= G_{er}^* \begin{pmatrix} I \\ \tau\Delta_{el} \end{pmatrix}^* \begin{pmatrix} X_e & Y_e \\ Y_e^T & U_e \end{pmatrix} \begin{pmatrix} I \\ \tau\Delta_{el} \end{pmatrix} G_{er} \end{aligned} \tag{15}$$

will be satisfied if

$$\begin{pmatrix} I \\ \tau\Delta_{el} \end{pmatrix}^* \begin{pmatrix} X_e & Y_e \\ Y_e^T & U_e \end{pmatrix} \begin{pmatrix} I \\ \tau\Delta_{el} \end{pmatrix} \succeq 0, \quad \forall \tau \in [0,1]. \tag{16}$$

It is easy to verify that robust stability of M against $\mathbf{\Delta}$ follows from robust stability of M_e against $\mathbf{\Delta_e}$. By applying the IQC stability theorem with the multipliers $\Pi_e = \begin{pmatrix} G_{er}^* X_e G_{er} & G_{er} Y_e G_{el} \\ G_{el}^* Y_e^T G_{er} & G_{el}^* U_e G_{el} \end{pmatrix}$, robust stability is reduced to a frequency domain inequality. With the KYP lemma we arrive at the following robustness test: M is robustly stable against $\mathbf{\Delta}$ if there exists an $F \in \mathbb{F}$ such that

$$R_L^T F R_L \prec 0, \tag{17}$$

where

$$R_L = \begin{pmatrix} I & 0 \\ A_L & B_L \\ C_L & D_L \end{pmatrix} \tag{18}$$

and

$$\mathbb{F} \triangleq \left\{ F = \left[\begin{array}{cc|cc} 0 & P & 0 & 0 \\ P & 0 & 0 & 0 \\ \hline 0 & 0 & X_e & Y_e \\ 0 & 0 & Y_e^T & U_e \end{array}\right] : \begin{array}{l} X_e \in \mathbb{S}^{n_e}, \\ U_e \in \mathbb{S}^{n_u}, \\ Y_e \in \mathbb{R}^{n_e \times n_u}, \\ P \in \mathbb{S}^d \end{array} \right\}. \tag{19}$$

Note that we choose G_i for $i = 1, \ldots, \nu$ as described by the minimal realization [23]

$$\left[\begin{array}{c|c} A_{G_i} & B_{G_i} \\ \hline C_{G_i} & D_{G_i} \end{array}\right] = \left[\begin{array}{ccccc|c} -p_i & 0 & \cdots & \cdots & 0 & 1 \\ 1 & -p_i & \ddots & \vdots & \vdots & 0 \\ 0 & 1 & \ddots & \ddots & \vdots & \vdots \\ \vdots & \ddots & \ddots & -p_i & 0 & \vdots \\ 0 & \cdots & \cdots & 1 & -p_i & 0 \\ \hline & & & 0 & & 1 \\ & & & I_{q_i} & & 0 \end{array}\right] \otimes I_{r_i}. \tag{20}$$

As a result, we arrive at $l_i = (q_i + 1) r_i$, and $k_i = q_i r_i$. We stress that the choice of q_i influences the McMillan degree of G_i and hence the size of the LMI (17).

B. Stability test for time-varying parametric uncertainties

Motivated by our setup, let us now consider the set $\mathbf{\Delta}$ defined by the following structured time-varying repeated parametric uncertainties:

$$\Delta_r(t) = diag(I_{r_1} \otimes \delta_1(t), ..., I_{r_\nu} \otimes \delta_\nu(t)).$$

It is assumed that the value of the parameter $\delta_j(t)$ and its rate-of-variation $\vartheta_j(t) = \dot{\delta}_j(t)$ are contained in the hyper-rectangular region

$$\mathcal{R}_j = \left\{(x_j, y_j) : x_j \in [\underline{\delta}_j, \overline{\delta}_j], y_j \in [\underline{\vartheta}_j, \overline{\vartheta}_j]\right\} = co\,\mathcal{R}_j^c \quad (21)$$

where $\underline{\delta}_j \leq 0 \leq \overline{\delta}_j$, $\underline{\vartheta}_j \leq 0 \leq \overline{\vartheta}_j$ and

$$\mathcal{R}_j^c = \left\{(\delta_j^{(1)}, \vartheta_j^{(1)}),\ (\delta_j^{(2)}, \vartheta_j^{(2)}),\ (\delta_j^{(3)}, \vartheta_j^{(3)}),\ (\delta_j^{(4)}, \vartheta_j^{(4)})\right\}$$

for $j = 1, ..., \nu$, as depicted in Fig. 7.

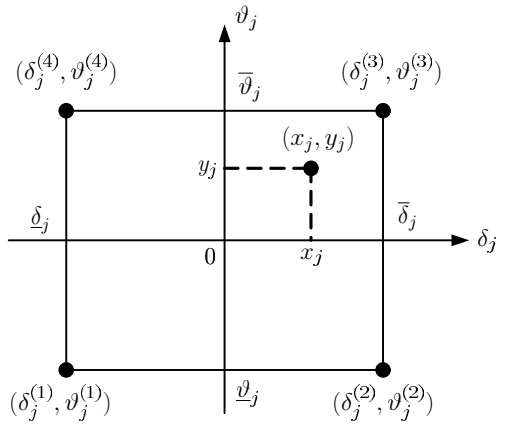

Fig. 7. The region of variations $\mathcal{R}_j$.

With $\Delta_{el}^i \triangleq \text{diag}(I_{l_1} \otimes \delta_1^{(i)}, ..., I_{l_\nu} \otimes \delta_\nu^{(i)}, I_{k_1} \otimes \vartheta_1^{(i)}, ..., I_{k_\nu} \otimes \vartheta_\nu^{(i)})$ for $(\delta_j^{(i)}, \vartheta_j^{(i)}) \in \mathcal{R}_j^c$, the robust stability test can be formulated as follows.

Theorem 2 ([23]): M is robustly stable against $\mathbf{\Delta}$ if there exists $F \in \mathbb{F}$ with $R_L^T F R_L \preceq 0$ and

$$U_{e_{11}} \preceq 0, \quad U_{e_{22}} \preceq 0, \quad \begin{pmatrix} I \\ \Delta_{el}^i \end{pmatrix}^T \begin{pmatrix} X_e & Y_e \\ Y_e^T & U_e \end{pmatrix} \begin{pmatrix} I \\ \Delta_{el}^i \end{pmatrix} \succeq 0 \quad (22)$$

for all $(\delta_j^{(i)}, \vartheta_j^{(i)}) \in \mathcal{R}_j^c$, $j = 1, \ldots, \nu$. Here $U_{e_{11}}$ and $U_{e_{22}}$ denote the left-upper and right-lower diagonal blocks of U_e of dimensions $\sum_{i=1}^{\nu} l_i$ and $\sum_{i=1}^{\nu} k_i$ respectively.

For proving this result, it suffices to observe that the validity of (22) at the generators $\mathcal{R}_j^c$ for $j = 1, \ldots, \nu$ implies (16) for arbitrary parameter curves $(\delta_j(t), \vartheta_j(t)) = (\delta_j(t), \dot{\delta}_j(t))$ that are contained in the full polytope $\mathcal{R}_j$ for $j = 1, \ldots, \nu$.

TABLE II
STABILITY MARGINS

Tests	Uncertainties	Ranges of variation	Rates
1	L_s	$90.50\% - 111.73\%$	$0 - 0.645$
2	L_r	$90.50\% - 111.72\%$	$0 - 0.042$
3	L_m	$92.50\% - 105.10\%$	$0 - 0.033$
4	ω_m	$26.5\% - 173.5\%$	$0 - 600000$
5	L_s and ω_m		
	L_s	$91\% - 109\%$	$0 - 0.01$
	ω_m	$65\% - 135\%$	$0 - 125$
6	L_r and ω_m		
	L_r	$90.50\% - 109.50\%$	$0 - 0.01$
	ω_m	$65.00\% - 135.00\%$	$0 - 250$
7	L_m and ω_m		
	L_m	$93\% - 105\%$	$0 - 0.01$
	ω_m	$65\% - 135\%$	$0 - 125$

C. Stability margin with rates of variation

Based-on the configuration as shown in Fig. 5 we can easily construct the standard configuration as in Fig. 6 for testing robust stability of the LPV-controlled system within the above given IQC-framework.

For this purpose, we describe the machine inductances, the rotor mechanical speed ω_m and their variations as uncertainties in a convex hull as in (21). The result in Theorem 2 is then implemented with the help of YALMIP, a toolbox [25] for rapid prototyping of optimization problems. The obtained results are summarized in Table II. For the purpose of investigating the stability margin of the controlled system in the face of only one parameter variation, the tests 1, 2, 3, and 4 are performed for L_s, L_r, L_m, ω_m, and their variations, respectively. The LFR form of the closed-loop system is constructed with the help of the robust control toolbox, while the corresponding region-of-variation (21) is re-constructed for each of the respective parameter variations. The results show that the closed-loop system remains stable when L_s varies from 90.5% to 117.33% of its nominal value while its rate varies in $[0, 0.645]$. The same conclusions are drawn, with the respective numerical results in Table II, for variations in L_r, L_m and ω_m respectively. Note that the stability region for the mechanical rotor speed ω_m is quite large, even if allowing for very fast variations. This is indeed consistent with the controller design algorithm which is based on the assumption that there are no bounds on the rate-of-variation. The tests 5, 6, and 7 are performed in the same fashion but for the uncertainties of ω_m in combination with L_s, L_r, and L_m, respectively. It is interesting to observe that, in these cases, the stability of the system is no longer guaranteed for arbitrary fast variation of the mechanical rotor speed ω_m. Its rate-of-variation has to be decreased to $[0, 125]$ in the tests 5, 7 and to $[0, 250]$ in the test 6, respectively, while its range-of-variation decrease to $[65\%, 135\%]$. Still, these margins for the mechanical rotor speed ω_m are in line with the practical need of tolerating up to $[70\%, 130\%]$ of its nominal synchronous speed value.

These analysis results also confirm the reliability of the DFIG with the designed LPV controller in the real experimental setup as presented in Section II.

V. Conclusion

This paper presents IQC analysis results for a LPV-controlled doubly-fed induction generator. The design of the LPV current controller is relying on the nominal model of the doubly-fed induction generator, and it is based on viewing the online measurable mechanical angular speed of the rotor as a time-varying parameter. Robust stability of the controlled system is tested by considering the machine inductances and the rotor's mechanical angular speed as slowly time-varying parameters. This analysis has been performed based on the IQC framework which allows to include bounds on both the values and the rate-of-variation of the parameters. Robustness margins have been given to prove that the controlled system remains stable in face of slowly time-varying parametric uncertainties of the machine.

Acknowledgment

The first author would like to thank the Vietnamese Government for the financial support through the project 322.

The authors are especially grateful to Dr. Volkmar Müller at the Institute of Electrical Power Engineering, faculty of Electrical Engineering and Information Technologies, Dresden University of Technology, Germany, for allowing to carry out the experiments and for his very kind hospitality. Special thanks go to Dr. Phung Ngoc Lan and Nguyen Tran Duc Viet for their assistances during the experimental work. Finally, we are grateful to to Dr. Hakan Koroglu at Delft Center for Systems and Control, Delft University of Technology, The Netherlands, for many useful discussions and also for his help to implement the IQC test in Matlab.

Appendix

Doubly-fed induction machine parameters referred to the stator side:

Rated power	$4kW$
Stator voltage	$230/400V$ (Δ/Y)
Rotor voltage	$950V$
Rotor current	$2.7A$
Rated speed	$1440rpm$
Moment of inertia	$0.032kgm^2$
Stator resistance	$R_s = 1.070\Omega$
Rotor resistance	$R_s = 1.32\Omega$
Stator leakage inductance	$L_{\sigma s} = 0.0066H$
Rotor leakage inductance	$L_{\sigma r} = 0.0098H$
Mutual inductance	$L_m = 0.1601H$

References

[1] H. Miyagi Y. Long and K. Yamashita. Windmill power systems controller design using H_∞ theory. *IEEE International Conference on Systems, Man, and Cybernetics*, 5:3490–3495, 2000.

[2] C. Wang and G. Weiss. Self-scheduled LPV control of a wind driven doubly-fed induction generator. *IEEE Conference on Decision and Control*, pages 1246–1251, Dec 2006.

[3] D. Fodor and R. Toth. Speed sensorless linear parameter variant H_∞ control of the induction motor. *IEEE Conference on Decision and Control*, 4:4435– 4440, 2004.

[4] E. Prempain, I. Postlethwaite, and A. Benchaib. A linear parameter variant H_∞ control design for an induction motor. *Control Engineering Practice*, 10:633–644, 2002.

[5] S. George and M. Rita. Loop-shaping H_∞ control for a doubly fed induction motor. *12th European Conference on Power Electronics and Applications*, page CDROM, 2007.

[6] J.D. Bendtsen and K. Trangbaek. Discrete-time LPV current control of an induction motor. *IEEE Conference on Decision and Control*, 6:5903–5908, Dec 2003.

[7] K. Trangbek. *Linear Parameter Varying Control of Induction Motors*. PhD thesis, Aalborg University, Denmark, 2001.

[8] S.Peresada, A.Tilli, and A.Tonielli. Robust output feedback control of a doubly-fed induction machine. *IEEE Annual Conference of industrial Electronics Society IECON99*, pages 1348–1354, 1999.

[9] E. Laroche, Y. Bonnassieux, H. Abou-Kandil, and J. P. Louis. Controller design and robustness analysis for induction machine-based positioning system. *Control Engineering Practice*, 12:757–767, Jun 2004.

[10] P. Gahinet, P. Apkarian, and M. Chilali. Affine parameter-dependent lyapunov functions and real parametric uncertainty. *IEEE Transactions on Automatic Control*, 41:436–442, Mar 1996.

[11] W. M. Haddad and V. Kapila. Robust stabilization for continuous-time systems with slowlytime-varying uncertain real parameters. *IEEE Transactions on Automatic Control*, 43:987–992, Jul 1998.

[12] A. Megretski and A. Rantzer. System analysis via integral quadratic constraints. *IEEE Transactions on Automatic Control*, 42:819–830, 1997.

[13] A. Helmerssonn. An IQC-based stability criterion for systems with slowly varying parameters. *14th World Congress of IFAC, Beijing, China*, pages 525–530, Jul 1999.

[14] H. Nguyen Tien, C. W. Scherer, and J. M. A. Scherpen. Discrete-time linear parameter varying control of doubly-fed induction generators. *International Advanced Symposium on Electrical, ISEE2007, VietNam*, pages 266–273, 2007.

[15] S. Peresada, A. Tilli, and A. Tonielli. Power control of a doubly fed induction machine via output feedback. *Control Engineering Practice*, 12:41 – 57, 2004.

[16] H. Nguyen Tien, C. W. Scherer, and J. M. A. Scherpen. Robust performance of self-scheduled LPV control of doubly-fed induction generator in wind energy conversion systems. *12th European Conference on Power Electronics and Applications, EPE2007, Aalborg, Denmark*, page CDROM, 2007.

[17] P. Gahinet, A. Nemirovski, A. J. Laub, and M. Chilali. *LMI Control Toolbox for use with Matlab*, volume 1. The Mathworks, 1995.

[18] R. Ottersten. *On Control of Back-to-Back Converters and Sensorless Induction Machine Drives*. PhD thesis, Chalmers University of Technology, 2003.

[19] G. Balas, R. Chiang, A. Packard, and M. Safonov. *Robust Control Toolbox*. The Mathworks, 2006.

[20] A. Helmersson. *Methods for robust gain scheduling*. PhD thesis, Linkoping University, 1995.

[21] J. S. Shamma. Robust stability with time-varying structured uncertainty. *IEEE transaction on Automatic control*, 39:714–724, 1994.

[22] H. Koroglu and C. W. Scherer. Robust stability analysis for structured uncertainties with bounded variation rates. *16th IFAC World congress*, Jun 2005.

[23] H. Koroglu and C. W. Scherer. Robust stability analysis against perturbations of smoothly time-varying parameters. *IEEE Conference on Decision and Control*, pages 2895 – 2900, 2006.

[24] U. Jonsson and A. Rantzer. Systems with uncertain parameters-time-variations with bounded derivatives. *IEEE Conference on Decision and Control*, 3:3074–3079, Dec 1994.

[25] J. Lofberg. YALMIP: a toolbox for modeling and optimization in matlab. *IEEE International Symposium on Computer Aided Control Systems Design, Taipei, Taiwan*, pages 284–289, 2004.